Beneficial rhizobacteria Pseudomonas simiae WCS417 induces major transcriptional changes in plant sugar transport

Antoine Desrut, Bouziane Moumen, Florence Thibault, Rozenn Le Hir, Pierre Coutos-Thévenot, Cécile Vriet

BENEFICIAL RHIZOBACTERIA *PSEUDOMONAS SIMIAE* WCS417 INDUCES MAJOR TRANSCRIPTIONAL CHANGES IN PLANT SUGAR TRANSPORT

Antoine Desrut[1], Bouziane Moumen[1], Florence Thibault[1], Rozenn Le Hir[2], Pierre Coutos-Thévenot[1], Cécile Vriet[1]

[1]Laboratoire Ecologie et Biologie des Interactions, UMR CNRS 7267, Université de Poitiers, 86073 Poitiers Cedex 9, France.

[2] Institut Jean-Pierre Bourgin, INRA, AgroParisTech, CNRS, Université Paris-Saclay, 78000 Versailles, France.

Email adresses of the authors

Antoine Desrut : antoine.desrut@univ-poitiers.fr ; Bouziane Moumen : Bouziane.Moumen@univ-poitiers.fr ; Florence Thibault florence.thibault@univ-poitiers.fr ; Rozenn Le Hir : rozenn.le-hir@inrae.fr ; Pierre Coutos-Thévenot : Pierre.Coutos@univ-poitiers.fr

Corresponding Author

Cécile Vriet

UMR7267 EBI, Poitiers, France

Email : cecile.vriet@univ-poitiers.fr

Tel: +33 (0)5 49 45 48 48

Highlight

The plant sugar transporters SWEET11 and SWEET12 are functionally involved in the interaction between *Arabidopsis thaliana* and the plant growth promoting rhizobacteria *Pseudomonas simia*e WCS417.

Abstract

Plants live in close relationships with complex populations of microorganisms, including rhizobacteria species commonly referred to as Plant Growth Promoting Rhizobacteria (PGPR). PGPR are able to confer to plants an improved productivity but the molecular mechanisms involved in this process remain largely unknown. Using an *in vitro* experimental system, the model plant *Arabidopsis thaliana*, and the well characterized PGPR strain *Pseudomonas simia*e WCS417, we have carried out a comprehensive set of phenotypic and gene expression analyses. Our results show *Ps*WCS417 induces major transcriptional changes in sugar transport and in other key biological processes linked to plant growth, development and defense. Notably, we identified a set of 13 genes of the SWEET and ERD6-like sugar transporter gene families whose expression is up- or down-regulated in response to the seedling root inoculation with the PGPR or exposure to its volatile compounds. Using a reverse genetic approach, we demonstrate that SWEET11 and SWEET12 are functionally involved in the interaction and its plant growth promoting effects, possibly by controlling the amount of sugar transported from the shoot to the root and to the PGPR. Altogether, our study reveals PGPR-induced benefical effects on plant growth and development are associated with changes in plant sugar transport.

Key words

Plant-microbe interaction, Plant Growth Promoting Rhizobacteria, *Arabidopsis thaliana*, *Pseudomonas simiae*, Sugar transport, SWEET, ERD6-like.

INTRODUCTION

In the rhizosphere, plants establish close relationships with a diverse set of non-pathogenic rhizobacteria species, commonly named PGPR for Plant Growth Promoting Rhizobacteria (PGPR). PGPR are known to stimulate plant productivity, either directly, by producing phytohormones, volatile compounds and/or by improving the plant nutrient acquisition (phosphate solubilization, nitrogen fixation, siderophore production and iron uptake), or indirectly by conferring to the host plant an enhanced protection against various abiotic and biotic stresses (Vacheron et al. 2013). Their biocontrol activity is achieved by a direct antagonism and/or competition for nutrients against soil pathogens, and by the production of antimicrobial substances, some of them volatiles. Some PGPR are also able to stimulate the plant defenses against leaf pathogens by a process called Induced Systemic Resistance (ISR) (Pieterse et al. 2014). Taking into account their beneficial effects on plant productivity, PGPR may contribute to the development of a more sustainable agriculture system. However a better understanding of the molecular mechanisms involved in plant-PGPR interaction is needed before they can be widely used in agriculture (Vacheron et al. 2013).

A growing body of evidence demonstrates the importance of sugar transport in plant pathogen resistance and in plant-microorganism mutualistic symbioses (Bezrutczyk et al. 2018; Hennion et al. 2019). In contrast, the role and regulation of sugar transport in plant-PGPR interactions remain to be investigated. PGPR promotes plant growth and in return may receive carbohydrate or other resources, notably as root exudates, from the host plant photosynthetic activity and source-to-sink carbon partitioning. Possibly these processes may involve PGPR-induced changes in plant sugar transport and metabolism that could lead to a regulated pool of sugars available for the PGPR, and may play a role in the efficiency of the interaction. In favor of these hypotheses, *Ps*WCS417r mutants that were unable to utilise carbohydrate sources displayed reduced root colonisation fitness (Cole et al. 2017). However, very few studies to date have investigated whether changes in plant carbon allocation occur during plant-PGPR interactions (Miotto-Vilanova et al. 2016; Schwachtje et al. 2011).

Sugars are the primary products of photosynthesis and serve as the primary energy source in plants. They are involved in many metabolic and signaling pathways controlling plant growth, development and stress tolerance. The transport and partitioning of sugars from source to sink organs through the phloem are major parameters controlling crop productivity. Many environmental factors, both biotic and abiotic, can affect this source-sink relationship (Lemoine et al. 2013). Sugars are transported across the plasma membrane or across the

membranes of various organelles and are loaded into - and unloaded from - the phloem, via a large number of sugar transporters. The Arabidopsis genome code for 79 sugar transporter proteins: (i) 53 Monosaccharide Transporters (MST), including 14 Sugar Transporter Protein (STP) and 19 sugar transporters named "ERD6-like" (named after the Early Responsive to Dehydration *ERD6* gene, the least investigated sub-group to date; (ii) Nine sucrose transporter proteins called SUT or SUC; and (iii) 17 sugar facilitator proteins named SWEET ("Sugar Will Eventually Be Exported Transporters") that transport mainly sucrose, glucose or fructose along an existing concentration gradient. Together with invertase enzymes, and other sugar-metabolism related proteins, these sugar transporters allow a fine-tuned regulation of sugar transport and supply to sink organs (Lemoine et al. 2013).

In order to identify plant genes playing an essential role in the efficiency of plant-PGPR interaction, and investigate the importance of plant sugar transport in this biological process, we have carried out detailed phenotypic and gene expression analyses on seedlings of *Arabidopsis thaliana* inoculated with the well characterized PGPR strain *Pseudomonas simia*e WCS417r (Berendsen et al. 2015; Cole et al. 2017; Verhagen et al. 2010; Wintermans et al. 2016; Zamioudis et al. 2014; Zamioudis et al. 2015; Zamioudis et al. 2013). Results from our transcriptome and targeted gene expression analyses (by RNA-sequencing and qRT-PCR) show this strain notably induces major changes in the expression of several sugar transporter genes, including two sugar facilitators of the SWEET family, *SWEET11* and *SWEET12*. The expression of these two genes is down-regulated in the roots and shoots of Arabidopsis seedlings 7 days post inoculation of their roots with *Ps*WCS417r, and via the volatile compounds emitted by this strain. Furthermore, our reverse genetic analysis reveals a severe loss of the PGPR beneficial effects on plant growth and development in the *sweet11/sweet12* double mutant in comparison to the wild type. Lastly, results from our starch and sugar content measurements and histochemical analyses indicate SWEET11 and SWEET12 might control the outcome of plant-PGPR interaction through their possible function in sucrose phloem loading in shoots and unloading in roots. Altogether, our findings suggest PGPR-induced beneficial effects on plant growth and development may involve changes in plant sugar transport and carbon resource allocation.

MATERIALS AND METHODS

Biological material

Plant material and growth conditions

Arabidopsis thaliana (Arabidopsis) ecotype Columbia (Col-0) was used as model plant species in this study. The Arabidopsis single mutant lines *sweet11-1* (SALK_073269.20.35.x) and *sweet12-1* (SALK_031696.56.00.x) carry a T-DNA insertion in the *SWEET11* and *SWEET12* genes, respectively. These lines were originally obtained from the European Arabidopsis Stock Centre (http://arabidopsis.info/) and previously reported to be knock-out lines (Chen et al. 2012). The *sweet11-sweet12* double mutant and the *pSWEET11:GUS* and *pSWEET12:GUS* lines have been generated and characterized as described earlier (Le Hir et al. 2015).

For *in vitro* culture, Arabidopsis seeds were surface sterilized for 5 min in 5 % (v/v) hypochlorite and 0.1 % Tween®20 detergent solution, and washed five times in sterile water. Seeds were sown in sterile Petri-dishes (140x140x20,6 mm) on half strength (0,5x) Murashige and Skoog (MS) medium (M0222, Duchefa Biochemie, Haarlem, The Netherlands), without sucrose, supplemented with 0.5 % of MES (Morpholino-Ethane-Sulfonic acid monohydrate; MW=213,2 $gmol^{-1}$) (ACROS Organics™, 172591000) and 0.8 % (w/v) of plant Agar Type A (Sigma-Aldrich®, A4550), pH 5.7. The plates containing 10 seeds each were sealed with two layers of parafilm. After two days of seed stratification at 4 °C in the dark, the plates were positioned vertically in a growth chamber (MLR 351H or 352H SANYO/Panasonic equipped with the fluorescent lamps FL40SSW/37 from PANASONIC or equivalent: 36W-840 from ORTES) under a long-day photoperiod (16h of light), with a light intensity of 120-140 $\mu mol.m^{-2}.s^{-1}$, and at a temperature of 22 °C. Seedlings were grown for five days in these growth conditions prior their co-cultivation with the rhizobacteria.

Rhizobacteria strain and cultivation

The plant growth promoting rhizobacteria (PGPR) strain *Pseudomonas simiae* WCS417r (gift from C.M.J. Pieterse, Utrecht University, Netherland) was used in this study. Glycerol stocks (with 40% glycerol) of the rhizobacteria were prepared from overnight cultures of WCS17r in LB medium (low salt) containing 10 $g.L^{-1}$ tryptone (Biokar, A1401HA), 5 $g.L^{-1}$ yeast extract (Biokar, A1202HA), 5 $g.L^{-1}$ NaCl (Fischer Scientific, 5312071), pH 7.2, and supplemented with 50 $\mu g.mL^{-1}$ of Rifampicin. Glycerol stocks were stored at -80 °C.

Preparation of the inoculum and inoculation of Arabidopsis seedlings with the PGPR *Ps*WCS417r

Preparation of the inoculum

For preparation of the inoculum, an aliquot of a glycerol stock of *Ps*WCS417r was streaked on solid King B medium (KB) containing 20 $g.L^{-1}$ Bacto™ Peptone (Difco™, 211677), 1.5 $g.L^{-1}$ Dipotassium Phosphate (Sigma-Aldrich®, P-5504), 1.5 $g.L^{-1}$ Magnesium Sulfate (ACROS Organics™, 124900010), 15 $g.L^{-1}$ Bacteriological agar type E (Biokar, A1012HA), pH 7.2, and supplemented with 50 $\mu g.mL^{-1}$ of Rifampicin. After 24 h at 28 °C, bacterial cells were collected in 10 mM $MgSO_4$, washed twice with 50 mL of 10 mM $MgSO_4$ by centrifugation for 5 min at 5000 *g*, and resuspended in 50 mL of 10 mM $MgSO_4$. The bacterial titer was adjusted to an OD_{600nm} of 0.002 to obtain an inoculum with a bacterial density of 2.10^6 colony-forming $units.mL^{-1}$ ($CFU.mL^{-1}$). For all experiments, this bacterial density was confirmed by counting the number of CFU on KB medium.

Inoculation of Arabidopsis seedlings with the PGPR in physical contact with their roots

Five days after seed sowing, Arabidopsis seedlings (10 per plates) were inoculated with 10 µL of *Ps*WCS417r at 2.10^6 $CFU.mL^{-1}$ (in 10 mM $MgSO_4$ solution) in physical contact with their roots, at 1 cm under the shoot-root junction (Fig. S1). For the mock treatment, seedlings were treated the same way with a 10 mM $MgSO_4$ solution. The plates were sealed with two layers of parafilm and transferred back to the plant growth chamber.

Treatment of Arabidopsis seedlings with the volatile organic compounds emitted by the PGPR

One hundred µL of *Ps*WCS417r at 2.10^6 $CFU.mL^{-1}$ (in 10 mM $MgSO_4$ solution) were spotted on solid LB medium [low salt; 10 $g.L^{-1}$ tryptone (Biokar, A1401HA), 5 $g.L^{-1}$ yeast extract (Biokar, A1202HA), 5 $g.L^{-1}$ NaCl (Fischer Scientific, 5312071), 15 $g.L^{-1}$ Bacteriological agar type E (Biokar, A1012HA), pH 7.2] into a small Petri dish (35x35x10mm) itself placed inside a larger Petri dish (140x140x20,6 mm) containing the 5 day old Arabidopsis seedlings (10 per plate). In this experimental setting, the seedlings were physically separated from the inoculum but gas exchange was allowed between the two compartments (Fig. S1). For the mock treatment, the inoculum was replaced by a 10 mM $MgSO_4$ solution. The plates were sealed with two layers of parafilm and transferred back to the plant growth chamber.

Phenotypic analyses

Root and shoot biomass measurement

For shoot and root fresh weight measurements, seedlings were sectioned at the root/shoot junction, and the weight (pool of 3 to 10 individuals) immediately measured on an analytical balance.

Phenotypic analysis of root system architecture

For primary and lateral root analyses, digital images of Arabidopsis seedlings were taken using a digital camera (D5200 Nikkon equipped with a AF 90 mm 1:2.8 Macro 1:1 TAMRON lens). For root hair analyses, digital images of the primary root tips were acquired using a macroscope (Macro View MVX10 Olympus) with a 20 fold magnification. The ImageJ software (Schneider et al. 2012) equipped with the SmartRoot plugin (Lobet et al. 2011) was used to measure the primary and lateral root lengths, and root hair length and density on a 1 mm^2 segment located at 1 mm above the root tip. Unless otherwise indicated, data are means ± the standard error of the mean (SEM) of 9 biological replicates from 3 independent experiments.

Total RNA extraction

Plant samples for gene expression analysis were harvested at mid-day (8h of light, 16h photoperiod), 7 days post inoculation unless otherwise indicated. Roots and shoots of Arabidopsis seedlings were harvested separately by sectioning the root-shoot junction, immediately frozen in liquid nitrogen, and stored at -80 °C. Total RNA was extracted from 25-100 mg of shoot and root tissues using a phenol/chloroform extraction procedure adapted from Box et al. (2011). Briefly, frozen tissues were grinded using a TissueLyser II (Qiagen) bead mill (30 Hz; 30 sec). Total RNA was extracted with 0.5 mL of RNA extraction buffer solution (25 mM Tris-HCl (pH 8); 25 mM EDTA; 75 mM NaCl; 2 % (w/v) SDS; 7.8 % (v/v) β-Mercaptoéthanol) and 0.5 mL of Phenol/Chloroform/Isoamyl Alcohol solution (25:24:1, v/v/v). Samples were vortexed for 30 sec and centrifuged 15 min at 13 200 *g* at 4 °C. The aqueous upper phase was recovered, transferred to new tubes and an equal volume (0.4 mL) of Chloroform/Isoamyl Alcohol (24:1; v/v) was added. Samples were then centrifuged 5 min at 13 200 *g* at 4 °C and the aqueous layer was transfered to a new tube containing 0.4 mL of 4 M $LiCl_2$. Samples were precipitated overnight at 4 °C and centrifuged 20 min at 20 600 *g* at 4 °C. The supernatant was discarded and the RNA pellet was resuspended in 50 µL of Nuclease-free water (Promega). After re-suspension, 5 µL of Sodium-acetate (3 M) and 125 µL of ice-cold 96% (v/v) EtOH were added. Samples were then left 1 hour at -20 °C for RNA

precipitation. After centrifugation 20 min at 20 600 *g* at 4 °C, the supernatant was discarded and the pellet washed in ice-cold 70 % (v/v) EtOH by centrifugation 5 min at 20 600 *g* at 4 °C, and dried under a fume hood. The RNA pellet was finally re-suspended with 6-30 µL of Nuclease-free water and stored at -80 °C.

RNA was quantified by spectrometry at 260 nm using the Multiskan GO Thermo Scientific spectrophotometer equipped with a µDrop™ Thermo Scientific Plate. RNA integrity was checked by gel electrophoresis on an agarose gel and by a measure of the 260/280nm ratio. Samples for RNA-sequencing were also quantified using a Qubit® 2.0 fluorometer with the Qubit RNA BR Assay kit, and their integrity checked by using the MultiNA microchip electrophoresis system (Shimazu).

Transcriptional analysis by RNA-sequencing

Library preparation and RNA-sequencing

RNA-seq was performed on three biological replicates for each tissus (root and shoot) and condition (Mock- and *Ps*WCS417r-treated). RNA libraries were constructed with polyA selection using the NEBNext® Ultra RNA Library Prep kit and sequenced on an Illumina HiSeq4000 platform by the company Genewiz.

Data preprocessing

Read quality was checked using the FastQC software V0.11.5 (http://www.bioinformatics.babraham.ac.uk/projects/fastqc/). FastQC check was performed before and after each preprocess. Removal of sequencing adaptors was performed with Cutadapt package (Martin 2011). Reads shorter than 30 bp were discarded using the FASTX toolkit software (http://hannonlab.cshl.edu/fastx_toolkit/index.html by Hannon Lab). *In silico* rRNA depletion was performed using SortMeRNA (Kopylova et al. 2012). This step consisted in mapping reads against Silva 16S, 18S, 23S and 28S rRNA genes and Rfam 5.8S rRNA genes to filter all reads hitting these databases. Then the removal of low quality reads and possible remaining sequencing adaptors was performed with Trimmomatic (version 0.32) (Bolger et al. 2014).

Read mapping to the genome and differential gene expression analysis

Briefly, preprocessed reads from each library and each condition were mapped against the *Arabidopsis thaliana* reference genome Araport11 (Cheng et al. 2017) using the HISAT2 package (with -dta option) (Kim et al. 2015). SAMtools (Li et al. 2009), was used to sort and convert mapping files to BAM format. Expressed genes and transcripts were infered using StringTie (without assembly option) (Pertea et al. 2015). Matrix of read counts mapped was

generated using prepDE.py provided by StringTie package. DESeq2 package (Love et al. 2014) was used for differential expression analysis as described in the StringTie manual. A list of differential expressed genes (DEG) with the following thresholds: a false discovery rate (FDR) < 0.05 and a fold change ≥ 2 were used for further analyses.

Enrichment analysis of Differentially Expressed Genes (DEGs)

Annotation and enrichment information for the DEGs were obtained from the Gene Ontology (GO) (Berardini et al. 2004) and Kyoto Encyclopedia of Genes and Genomes (KEGG) (Kanehisa et al. 2017; Kanehisa and Goto 2000) databases, and MAPMAN software (Thimm et al. 2004).

Relative gene expression analysis by Quantitative, Real Time PCR (qRT-PCR)

DNAse treatment and cDNA synthesis

Total RNA was extracted as described above, treated with DNAse I (Sigma-Aldrich) and reverse transcribed using the M-MLV reverse transcriptase (Promega) with oligodT primers according to the manufacturer instructions.

Primer design

Primers for qRT-PCR were designed using the NCBI Primer-Blast software (Ye et al. 2012), with the following criteria: a primer size comprised between 18-25 bp, a GC % of 45-60 %, a melting temperature (T_m) between 58 and 63 °C, and a PCR product size of 50 to 200 bp. Moreover, preferences were given for primer pairs with low self complementarity that were exon-exon shuffling or intron spanning. Sequences of the primers used in this study, and efficiency of the primers for the selected candidate genes, are listed in Table S12.

Quantitative Real Time PCR (qRT-PCR)

Gene expression analyses were performed by qRT-PCR using the GoTaq qPCR MasterMix (Promega) according to the manufacturer instructions (1 X GoTaq® qPCR Master Mix, 0.33 µM of forward and reverse primer, and 5 µL of 10-fold diluted cDNA per well).

The amplification reaction was carried out using a 96-well plate thermal cycler (Mastercycler Realplex2, Eppendorf). The amplification program consisted of an initial denaturation step (2 min at 95 °C) followed by 40 cycles of amplification with two stages (15 sec at 95 °C, 1 min at 60 °C). The specificity of the amplification was checked with a melting curve analysis consisting of an initial denaturation step of 15 sec at 95 °C followed by an increasing temperature with a step of 0.1 °C, from 60 °C to 95 °C, for 20 min.

Target gene expression was normalized using the reference gene At4g26410 (Czechowski et al. 2005; Lemonnier et al. 2014) whose expression remained stable in all condition

evaluated (in the different tissues, time points, and following inoculation with the PGPR strain) according to the results obtained with a second reference gene: AtUPL7 (At3g53090). Results were expressed as relative gene expression values using the $2^{-\Delta Ct}$ method (Schmittgen and Livak 2008). Unless otherwise indicated, data are mean ± SEM of 4 biological replicates, each from an independent experiment.

Quantification of sugar and starch contents

Samples for soluble sugar (glucose, fructose, sucrose) and starch assays were harvested at mid day (8 h light). Sugars and starch were extracted from approximately 100 mg (fresh weight) of plant tissue (root and shoot) following three wash steps (1,5ml and twice with 0,5 ml) in methanol: chloroform: water (12:5:3, v/v/v). After centrifugation (2 min at 6000 g), supernatants containing soluble sugars were diluted with 0.6 volume of water, and centrifuged (2 min at 2500 g). The upper aqueous phase containing the solubles sugars were collected and evaporated (3-4 h at 50°C) with a concentrator (MiVac; Genevac). Solubles sugars were resuspended in 100 µL of milliQ water and quantified using the Sucrose/Frucrose/D-Glucose (K-SUFRG) Assay Kit (Megazyme) according to the manufacturer instructions. Starch content was quantified from the pellet obtained after the methanol: chloroform: water (12:5:3, v/v/v) extraction using the Total Starch HK Assay Kit (Megazyme) according to the manufacturer instructions.

Histochemical and microscopy analyses of GUS expression

Histochemical analysis of the β-glucuronidase (GUS) reporter enzyme activity was performed as follow: Seedlings were preincubated with 90% (v/v) acetone for 30 min at -20°C, washed twice in 50 mM sodium phosphate (NaP) buffer at pH 7.0 for 10 min, and infiltrated with X-Glu reaction buffer (NaP buffer, 50mM ; K4[Fe(CN)6], 0.5 mM ; K3Fe(CN)6, 0.5 mM ; 5-bromo-4-chloro-3-indolyl-β-d-glucuronic acid, 1 mM ; Triton X100, 0.1%) under vacuum for 5 min. After 3 h incubation in dark at 37°C, seedlings were washed in 50 mM NaP buffer at pH 7.0 for 10 min and dehydrated successively in 96% and 70% ethanol. Following ethanol-dehydration (10 min incubation in ethanol 95° and 100°), root samples were embedded in LRW resin (24h at 60°C) and cut into 1,5 µm sections using an Ultramicrotome (Leica, EMUC6). The sections were fixed on glass slides and treated with Shiff reagent before to be imaged by a microscope (LEICA DM500 equipped with an ICC50 W camera) under bright-field illumination. Whole seedlings were imaged using a Leica Aperio-Versa microscope.

Statistical analyses

Statistical analyses of differences for morphological traits and relative gene expressions were carried out using a non-parametric Mann-Whitney-Wilcoxon test ($n < 30$) unless otherwise indicated. Tests were performed using the software GraphPad Prism version 7.0.

RESULTS

The plant growth promoting rhizobacteria *Pseudomonas simiae* WCS417r induces major transcriptional changes in biological processes linked to plant growth, development and defense.

Using the model plant species *Arabidpsis thaliana* and the PGPR *Pseudomonas simiae* we have set up an *in vitro* gnobiotic experimental system to study the PGPR modes of action and molecular mechanisms involved in their beneficial effects on plant growth and development (Fig. S1). Two experimental conditions of inoculation were tested: (i) in physical contact with the plant roots, and (ii) *via* the emission of volatile compounds only. Using this system, we carried out quantitative phenotypic analyses on a comprehensive set of plant growth and development parameters (Fig. 1). Our results show *Ps*WCS417r leads to strong positive changes in root and shoot biomasses and in several root architecture traits (primary and lateral root length, lateral root number, root hair length and density) 4, 7 and 10 days post inoculation (dpi) of 5 day old Arabidopsis seedlings (Fig. 1). Noteworthy, the PGPR effects were more marked on the root than on the shoot biomass (at 7 dpi, the root-to-shoot ratio increased from 0.19 to 0.35 in response to the PGPR) (Fig. 1 and Table S1). Unless otherwise indicated, we chose the time point 7 dpi for further analyses, however, positive effects of the PGPR on the seedling shoot and root biomasses were measured at 4 dpi and tended to increase with a longer co-cultivation period (10 dpi) (Fig. 1).

With the aim to identify genes involved in plant-PGPR interaction, we performed a genome-wide gene expression analysis by RNA-sequencing on root and shoot tissues of Arabidopsis seedlings, 7 days post inoculation of their roots with *Ps*WCS417r. Following quality control checks and filtering steps (Table S2), reads were mapped on the *Arabidopsis thaliana* reference genome Araport11 (Cheng et al. 2017) and subjected to a differential gene expression analysis (Table S3). Transcripts whose expression was up-regulated or down-regulated more than two fold in comparison to the mock treatment and with a FDR < 0.05, thereafter referred as Differentially Expressed Genes (DEGs), were selected for further

analyses (Fig. S2 and Table S4). The Venn diagram analysis we performed reveals *Ps*WCS417r induces differential gene expression changes between root and shoot tissues (out of all up- and down-regulated genes, only 11.2 % and 6.4 % were up-regulated and down-regulated, respectively, in both tissues). Furthermore, a set of 20 genes were either up-regulated in root and down-regulated in shoot, or vice versa (Fig. 2 and Table S5).

In order to gain insights into the biological processes linked to the PGPR plant growth promoting effects, we carried out functional enrichment analyses for the DEGs. We found *Ps*WCS417r induces major changes in the expression of genes involved in several hormonal pathways not only linked to plant growth and development, but also to abiotic and biotic stress responses (Fig. 2, Fig. S3 and Table S6-S9). Among the eight phytohormonal pathways studied, genes involved in the biosynthesis of Abscisic acid (ABA) and Salicylic acid (SA), and in the signaling pathways of Ethylene (ET), Jasmonic acid (JA) and Salicylic acid (SA) included the largest proportion (above 15%) of genes differentially expressed in response to *Ps*WCS417r (Table S7b). In contrast, very minor gene expression changes between the mock- and WCS417r-treated conditions were observed for a comprehensive set of photosynthesis-related genes, including genes encoding proteins of the photosystem I and II, Chl A-B-binding proteins, electron carriers, carbon fixation and chlorophyll biosynthesis proteins (Bang et al, 2008; KEGG pathway ath00195) (Table S3). Most of them were found highly expressed in shoot suggesting the seedlings were photosynthetically active in both conditions. Interestingly we also found that *Ps*WCS417r induced transcriptional changes for 24 genes encoding sugar and starch metabolism enzymes (Fig. 2d and Table S10). In plants, sucrose can be catabolized by either sucrose synthase (EC 2.4.1.1) or invertase (EC 3.2.1.26) enzymes. The Arabidopsis genome encodes 6 sucrose synthase genes (SUS) and 6 genes originally annotated as cell-wall invertases (CWIN). Among them, only the sucrose synthase genes SUS3 and SUS4 and the gene CWIN6, which was shown to have no invertase activity but instead function as a fructan exohydrolase (De Coninck et al, 2005), were transcriptionally regulated by the PGPR either in root and/or in shoot in our experimental conditions (Fig. 2d and Table S10).

_Ps_WCS417r transcriptionally regulate a set of 13 genes of the SWEET and ERD6-like sugar transporter gene families.

To further explore PGPR-induced changes in plant sugar transport and carbon resources allocation, we investigated the expression pattern of all 79 genes coding for sugar transporters in the Arabidopsis genome in our RNA-sequencing data and by qRT-PCR (Table S11 and Table S12). These genome-wide and targeted gene expression approaches led to the identification of a set of 14 sugar transporter genes that were differentially expressed in the mock- and PGPR-treated conditions, either in roots (6 genes : *SWEET3, SWEET11, SWEET12, ERD6-like13, ERD6-like15, and ERD6-like18)*) or in shoots (8 genes : *SWEET2, SWEET4, SWEET10, SWEET15, ERD6-like7, ERD6-like12, ERD6-like16 and INT2*) (Fig. S4). Noteworthy, all these genes, except one (an inositol transporter gene, *INT2*) belong to genes of the SWEET and ERD6-like families of sugar transporters, and the expression of most of them were found down-regulated by the PGPR. *ERD6-like13 and ERD6-like15* were the only two genes up-regulated in the root, and only the gene *SWEET10* was up-regulated in the shoot in response to inoculation with the *Ps*WCS417r (Fig. S4).

With the aim to submit a selected subset of these candidate genes to a reverse genetic approach and explore their functional implication in the efficiency of the plant-PGPR interaction, we extended the study of their expression profile to a kinetic analysis (at 4, 7, and 10 dpi) in response to the PGPR in physical contact with the seedling roots by real time, quantitative RT-PCR. In agreement with our transcriptomic data, the expression of all these 14 genes were statistically significantly induced or repressed at 7 dpi in physical contact condition. In this experimental condition, down-regulation of the genes *SWEET3, SWEET11, SWEET12* and *ERD6-like18* were at the highest at 4 dpi and remained relatively stable thereafter (at 7 and 10 dpi) in roots, whereas the genes *SWEET4, SWEET15* and *INT2* displayed the opposite trend in shoots (more strongly down-regulated from 7 or 10 dpi); a relatively stable expression over time was observed for the other candidate genes analysed (Fig. 3a and Table S13).

Next, we studied the phenotypic and gene expression effects of the PGPR *via* the emission of its volatile compounds only (ie. without physical contact with the plant roots). At 7 dpi, these latters led to a marked increase in the root and shoot biomasses and root architecture traits (except for the root hair density) of the wild type (WT) seedlings (Fig. 4 and Table S14). Noteworthy, these effects were even more marked than those observed when the PGPR was placed in physical contact with the Arabidopsis seedling roots (Fig. 1) suggesting an important role played by the volatile compounds emitted by *Ps*WCS417r on its plant growth

promoting activities. Regulation of the expression of only three out of the 14 candidate genes, namely *SWEET4*, *SWEET10* and *SWEET15* (in shoot), required a physical contact of the PGPR with the seedlings roots (Fig. 3, Table S13 and Table S15). Hence, transcriptional regulation mechanisms independent of the bacterial volatile compounds may be involved in these particular cases. On the opposite, at 7 dpi and in the roots, the genes *SWEET3*, *SWEET11*, *SWEET12* and *ERD6-like 18* were the most strongly down-regulated by the PGPR volatile compounds (Fig. 3b, Table S13 and Table S15).

SWEET11 and SWEET12 are functionally involved in plant-PGPR interaction and its plant growth promoting effects

In Arabidopsis, SWEET11 (At3g48740) and SWEET12 (At5g23660) belong to the clade III of the SWEET family. They are able to transport sucrose, glucose and fructose and are typically involved in cellular efflux processes (Chen et al. 2010; Chen et al. 2012; Eom et al. 2015; Le Hir et al. 2015). *SWEET11* and *SWEET12* may play a role in sucrose phloem loading and are involved in defense response to leaf pathogens (Chen 2014; Gebauer et al. 2017). These two genes are also known to be required for embryo development (Chen et al. 2015) and cell wall formation during vascular development (Le Hir et al. 2015). Lastly, transcript levels of *SWEET11* and *SWEET12* are up-regulated in leaves of plants exposed to water deficit, which may contribute to the increase in C export from the leaves to the roots observed in this abiotic stress condition (Durand et al. 2016). In roots, their role is still unknown but it has been suggested that these genes may be involved in the unloading of sucrose from the phloem to the root tissues (Durand et al. 2016).

To determine whether *SWEET11* and *SWEET12* are functionally involved in plant-PGPR interaction, we carried out the same set of phenotypic analyses than those performed on the WT (Fig. 1) on the single and double T-DNA insertion mutants of these two genes. These analyses were performed in response to the volatile compounds emitted by *Ps*WCS417r, the condition in which they were the most highly transcriptionally repressed by the PGPR at 7 dpi (Fig. 3). In axenic condition (mock treatment), only minor or no statistically significant differences were observed between the single loss-of-function mutants, the double mutant *sweet11/sweet12* and the WT for all the phenotypic traits analyzed. This also holds true for the *sweet11* and *sweet12* single mutants in presence of the PGPR (Fig. 4 and Table S14). In contrast, positive effects of *Ps*WCS417r volatile compounds on the root and shoot biomasses of the seedlings were strongly reduced (about two-fold less) in the double mutant *sweet11/sweet12* in comparison to the WT. Similarly, the beneficial effects of the PGPR

volatile compounds on the seedling primary and lateral root length and number were partially abolished. The root hair length and density were the only two root architecture traits for which no significant differences were observed between the double mutant and the WT in *Ps*WCS417r-treated condition (Fig. 4 and Table S14).

The detailed gene expression analysis we performed on the WT, single and double mutant lines reveals *SWEET11* and *SWEET12* were also transcriptionally repressed in response to the PGPR in shoot (1.6 and 2.6 fold down-regulation, respectively), albeit to a lower extent than in root (16.9 and 166.4 fold down-regulation, respectively) (Fig. 5). In addition, our results confirm the knock-out nature of the T-DNA insertions in these mutant lines in agreement with data in the literature (Chen et al, 2012). Moreover, inactivation of the *SWEET11* gene had no significant effects on the level and pattern of expression of the *SWEET12* gene, and *vice versa*, suggesting no compensation at the mRNA level exists between *SWEET11* and *SWEET12* (Table S15). We also studied the putative impact of the loss of expression of these two genes on the transcript levels of (i) the other WCS417r-transcriptionally regulated genes identified from our gene expression study, and (ii) the other SWEET genes belonging to the clade III of the SWEET family (*SWEET9* to *SWEET15*) (Eom et al. 2015). The candidate genes *SWEET3* in roots, and *SWEET2* and *ERD6-like16* in shoots were expressed at a lower level (4.2, 2.5 and 9.2 fold less expressed, respectively) in the double mutant than in the WT, whereas the clade III gene *SWEET13* in shoots followed the opposite trend of expression (10.3 fold more expressed in the double mutant than in the WT). Moreover, in response to the PGPR volatile compounds, the candidate genes *ERD6-like13* in roots, and *SWEET15* in shoots were significantly more transcriptionally regulated (2.4 fold less and 3.5 fold more, respectively) in the double mutant than in the WT (Fig. 5 and Table S15). Lastly, we investigated the expression of the three defense marker genes *PDF1.2*, *PR1* and *PAD3*. All three of them were strongly transcriptionally induced by *Ps*WCS417r volatile compounds in the WT (62.7, 46.5 and 15 fold increase) and single mutants, but induction of their expression was almost completely abolished in *sweet11/ sweet12* double mutant (Table S15).

_Ps_WCS417r-induced beneficial effects on plant growth and development are associated with changes in carbon resources allocation

In order to gain insight into the function of SWEET11 and SWEET12 in plant-PGPR interaction and its beneficial effects on plant growth and development, we investigated whether *Ps*WCS417r volatile compounds triggered changes in source-to-sink carbon partitioning in the WT and *sweet11/ sweet12* double mutant. Assessment of carbohydrate metabolism revealed that soluble sugar and starch contents were significantly elevated in the

shoots of WT seedlings exposed to *Ps*WCS417r volatile compounds (3.6, 4.9, and 23.1 fold increase in glucose, fructose and starch content, respectively) suggesting a reduced efflux of sugar toward the roots in presence of the PGPR. In non-inoculated seedlings soluble sugar contents were also significantly elevated in the shoots of *sweet11/sweet12* double mutant in comparison to the WT (3.9, 2.5, and 3.9 fold increase in sucrose, glucose, fructose content, respectively) (Fig. S5 and Table S16). Noteworthy, in response to *Ps*WCS417r volatile compounds, an even more pronounced increase in soluble sugar and starch contents than in the WT was observed in the shoot of *sweet11/sweet12* double mutant seedlings (5.6, 6, and 1.8 fold increase in glucose, fructose and starch content, respectively). In contrast, in roots, only minor or no statistically significant differences were observed between the two genotypes and upon exposure with *Ps*WCS417r volatile compounds (Fig. S5 and Table S16).

Taking into account the putative function of *SWEET11* and *SWEET12* in phloem unloading, we investigated the expression pattern of *SWEET12* in root, which of these two genes was the most highly expressed in this tissue. Histochemical analyses were carried out at 7 dpi on 12 day old *Arabidopsis thaliana* seedlings expressing the reporter gene GUS (β-glucuronidase) under the control of the native promoter of *SWEET12* (Fig. S6). A clear GUS signal could be observed in the root vascular system. More specifically in the roots, a strong GUS signal was found localized in lateral roots as well as in the elongation and differentiation/maturation zones for the primary root while almost no signal was observed at the root tip (Fig. S6a and S6b). Interestingly, in response to *Ps*WCS417r volatile compounds, a GUS signal could also be observed all along the primary and lateral roots, including at the primary root-lateral root junctions, which was not the case in the mock-treated condition (Fig. S6a and S6b). Furthermore, we analysed the localization of *SWEET12* gene expression in root sections (Fig. S6c). In seedlings exposed to *Ps*WCS417r volatile compounds, a GUS signal could be visualized in the root stele tissues, not only in the vacular tissues but also in the pericycle cells (Fig. S6c).

DISCUSSION

*Ps*WCS417r displays plant growth promoting activities that are accompanied by major transcriptional changes in sugar transport.

*Ps*WCS417r is a well characterized PGPR strain (Berendsen et al. 2015). However, the relative contribution of the volatile compounds emitted by *Ps*WCS417r to its plant growth promoting effects remained largely unknown to date. Our results reveal *Ps*WCS417r displays marked plant growth promoting activities, both in physical contact with seedling roots and via the production of volatile compounds only (Fig. 1 and Fig. 4). These results are in agreement with previous studies that were performed in a way *Ps*WCS417r could exert its effects via the production of diffusible and/or volatile compounds (Zamioudis et al. 2015; Zamioudis et al. 2013). *Ps*WCS417r grew better on LB medium than when placed in physical contact with the seedlings roots on MS medium, hence different concentration as well composition of volatile compounds may be produced between the two experimental conditions. Nevertheless, highly similar PGPR-induced plant growth promoting activities were observed in both systems (Fig. 1 and Fig. 4). These results suggest the volatile compounds emitted by WCS417r contribute to a large extent to its plant growth promoting activities.

Evidence in the literature suggests the compounds indole, 1-hexanol and pentadecane may be implicated in the plant growth promoting effects induced by PGPR (Blom et al. 2011). Indole in particular represents a good candidate since treatment of Arabidopsis seedlings with this volatile molecule lead to beneficial effects on shoot and root biomass and the root system architecture (Bailly et al. 2014) that are highly reminiscent to those obtained in response to inoculation with *Ps*WCS417r (Fig. 1 and Fig. 4). The two most prominent *Ps*WCS417-mediated alterations in root morphology are the stimulation of lateral root formation and root hair development. Auxin signaling and transport are known to play an important role in the PGPR-induced positive effects observed on these two traits (Zamioudis et al. 2015; Zamioudis et al. 2013). Remarkably, indole has been shown to participate in auxin-controlled lateral root initiation and development events beyond its role as auxin synthesis precusor, by interfering with auxin signaling (Bailly et al. 2014).

In our experimental system in which gas exchange with the outside is not allowed (sealed Petri dishes), CO_2 produced by the PGPR may also contribute to the plant growth promoting effects observed (Kai and Piechulla 2009). To shed light on this possibility, we checked the expression profile of *SUS3* (At4g02280), *GTP2* (At1g61800), *SUT4* (At1g09960) and *SWEET12* (At5g23660), four marker genes known to be induced in response to elevated CO2

(eCO_2) in Arabidopsis leaf tissues (Duan et al. 2014; Jauregui et al. 2015). In our experimental condition, the expression of these genes either remained unchanged or was repressed in response to *Ps*WCS417r (Table S3). Hence, an elevated CO_2 content due to bacterial growth does not seem to be responsible for the PGPR-induced beneficial effects observed on Arabidopsis seedling growth and development.

Both the genome-wide and targeted gene expression analyses we performed led to the identification of a set of 14 plant sugar transporter genes that were differentially expressed in the mock- and PGPR-treated conditions either in roots or in shoots (Fig. 3). Unexpectedly, all of these genes, except one, encode sugar facilitators of the SWEET and ERD6-like families, that transport sugars along the concentration gradient. The expression of most of them was found repressed by the PGPR at 7 dpi. *ERD6-like13* and *ERD6-like15* in roots, and *SWEET10* in shoots were the only three genes whose expression was found induced by *Ps*WCS417r (Fig. 3). In addition, it should be pointed out that the majority of these candidate genes were also transcriptionally regulated when the seedlings were solely exposed to the bacterial volatile compounds (Fig. 3).

A large and growing number of evidence in the literature exist regarding the effects PGPR can have on the concentration, signaling and metabolism of plant hormones, and the plant growth promotion triggered by PGPR may depend on these associated changes in phytohormone homeostasis (Tsukanova et al., 2017). Auxin signaling and transport in particular are known to play an important role in the PGPR-induced positive effects (Zamioudis et al. 2015; Zamioudis et al. 2013). In this study, we have explored the effects of PsWCS417r on the expression of genes of the phytohormone pathways in order to gain insights into the molecular mechanisms involved in its plant growth-promoting effects. Notably, this PGPR strain not only triggered transcriptional changes in the pathways of the plant growth-related hormones auxin, gibberellin and cytokinin but also in the biosynthesis and signaling pathways of abscisic acid, jasmonic acid (JA), ethylene (ET) and salicylic acid (SA), four phytohormones commonly implicated in plant responses to abiotic and biotic stress (Fig. 2, Fig. S3 and Table S7b). In addition, our qRT-PCR results confirm a transcriptional activation of a set of defense-marker genes both linked to the SA and JA/ET pathways in response to the PGPR, suggesting that, in our experimental conditions, this strain does not hold the ability to totally suppress the host immune responses. Altogether, these findings highlight the importance of plant defense responses in beneficial plant-PGPR interactions and suggest yet unknown molecular mechanisms may be at play in PGPR triggered plant growth-promoting effects.

The sucrose effluxers SWEET11 and SWEET12 are implicated in the plant growth promoting effects triggered by *Ps*WCS417r.

To date, very little is known regarding the nature and extent of the benefits plant-PGPR interactions confers to both partners. In particular, how the PGPR is perceived and whether it retrieve benefits from the interaction in exchange of its beneficial effects on plant growth and development are outstanding questions that remain to be answered. Most likely, these interactions are not static and may depend on environmental conditions and/or be species specific. Also, it should be kept in mind that in presence of the PGPR, and similarly to what has been shown in arbuscular mycorrhizal (AM) symbiosis and in plant-pathogen interactions (Bezrutczyk et al. 2018; Hennion et al. 2019), sugar transporter genes may be regulated (i) by the microbe to gain more sugars from the plant, or as part of its plant growth promoting effects, either directly or indirectly (eg via a positive effect on the photosynthetic activity), or (ii) by the plant to regulate the amount of sugars available for the microbe and its proliferation.

SWEET11 and SWEET12 are involved in phloem loading of sucrose (Chen et al. 2012) and it has been suggested they may also be involved in unloading of sucrose from the phloem to the root tissues (Durand et al. 2016). In order to investigate their functional role and importance in the efficiency of plant-PGPR interactions, we carried out a reverse genetic approach on these two candidate genes. Unexpectedly, our results revealed a severe loss of the PGPR beneficial effects in the double mutant in comparison to the wild type, suggesting that these genes play a functional role in the interaction and its plant growth promoting effects (Fig. 4). In addition, our results reveal an increase in soluble sugar and starch content was observed in shoots of the *sweet11/sweet12* mutants in comparison to the WT as well as in the PGPR-treated WT seedlings in comparison to non-inoculated controls. Morever, an even stronger increase in soluble sugar and starch content in shoots was observed in PGPR-treated *sweet11/sweet12* double mutant (Fig. S5).

Taking into account the putative function of SWEET11 and SWEET12 in sucrose phloem loading in leaves and unloading in roots, a reduced efflux of sugars from the leaves to the roots may be expected (i) in the WT in response to the PGPR volatile compounds given the transcriptional repression of *SWEET11* and *SWEET12* in this condition, and (ii) in non-inoculated *sweet11/sweet12* double mutant seedlings. Hence, SWEET11 and SWEET12 could play a role in controlling the amount of sugar transported from the shoot to the root to balance the needs of the host and its symbiont by limiting rhizobacterial proliferation.

However, assuming that a positive correlation exist between the efflux of sugars toward the root and the seedlings root growth and development, one might expect negative effects of the PGPR on these phenotypic traits in both WT and *sweet11/sweet12* mutant seedlings. Instead, we observed strong PGPR-triggered beneficial effects on the root biomass and architecture of the WT seedlings, and these effects were partially abolished in the double mutant (Fig. 4). Altogether, these results suggest that unknown indirect effects may be at play, and/or that the positive effects induced by the PGPR on the root architecture parameters may be more dependent on local changes in sugar fluxes in the roots than on global increase in source-to-sink carbon partitioning. In favor of this latter hypothesis, our histochemical analyses reaveled a tissue-specific expression pattern of the reporter gene GUS under the control of the native promoter of *SWEET12* gene in the primary root elongation and differentiation zones and in lateral roots. Importantly, in *Ps*WCS417r-treated seedlings a GUS signal could also be observed all along the roots and at the primary root-lateral root junctions (Fig. S6a and S6b). Furthermore, in cross sections of roots, an expression signal was observed in root stele tissues, both in the vacular tissues and in the pericycle (Fig. S6c), suggesting a role for SWEET12 in phloem unloading of sucrose toward root tissues, and in particular toward emerging lateral roots. Alternatively, SWEET11 and SWEET12 may play a role as a sensor. Additional experiments will be needed to further explore their role in response to PGPR. For instance, $^{14}CO_2$ pulse-chase experiments could be used to study dynamically long distance and local changes in sugar fluxes in response to the PGPR and should help refine the function of these two sugar transporters in the interaction and its plant growth promoting effects.

Lastly, further investigations into the function of the candidate genes identified in this study and their regulatory circuitry will identify additional factors essential for the outcome of plant-PGPR interactions. In the longer term, these novel insights should help develop innovative and environmentally friendly PGPR-based strategies for crop protection and productivity improvement, and contribute to the rise of a more sustainable agriculture.

DATA AVAILABILITY

Genetic locus identifiers of the genes presented in this study are listed in Table S12. All RNA-sequencing data related to the present study has been deposited to the National Centre for Biotechnology Information (NCBI) under the Bioproject accession number PRJNA559134.

ACKNOWLEDGEMENTS

This work was funded by the French Ministry of Higher Education, Research and innovation (AD, PhD grant), the 2015-2020 State-Region Planning Contracts (CPER), the European Regional Development Fund (FEDER), the Centre National de la Recherche Scientifique (CNRS) and the University of Poitiers. The IJPB benefits from the support of the LabEx Saclay Plant Sciences-SPS (ANR-10-LABX-0040-SPS). The authors would like to thank Pr. Corné Pieterse for the gift of the rhizobacteria strain *Ps*WCS417r. The authors gratefully acknowledge the ImageUP plateform, Bruno Merceron and Anne Cantereau for technical assistance in microscopy and macroscopy analyses. We also want to express our appreciation to students who contributed to this work, especially David Landry and Laurie Taylor. Lastly, we thank Dr. Rémi Lemoine for critical reading and revision of the manuscript.

AUTHOR CONTRIBUTION

Cécile Vriet: Conceptualization, Methodology, Investigation, Formal analysis, Visualization, Writing - Original draft preparation, Reviewing and editing. **Antoine Desrut:** Investigation, Formal analysis, Visualization, Writing - Original draft preparation. **Bouziane Moumen:** Software, Data curation, Formal analysis. **Florence Thibault:** Investigation. **Rozenn Le Hir:** Resources, Conceptualization, Validation, Writing - Reviewing and editing. **Pierre Coutos-Thévenot:** Validation, Supervision, Writing - Reviewing and editing. All authors approved the final manuscript.

REFERENCES

Bailly A, Groenhagen U, Schulz S, Geisler M, Eberl L, Weisskopf L (2014) The inter-kingdom volatile signal indole promotes root development by interfering with auxin signalling. The Plant journal : for cell and molecular biology 80: 758-771

Bang WY, Jeong IS, Kim DW, Im CH, Ji C, Hwang SM, Kim SW, Son YS, Jeong J, Shiina T, Bahk JD (2008) Role of Arabidopsis CHL27 protein for photosynthesis, chloroplast development and gene expression profiling. Plant Cell Physiol. 49:1350-63.

Berardini TZ, Mundodi S, Reiser L, Huala E, Garcia-Hernandez M, Zhang P, Mueller LA, Yoon J, Doyle A, Lander G, Moseyko N, Yoo D, Xu I, Zoeckler B, Montoya M, Miller N, Weems D, Rhee SY (2004) Functional annotation of the Arabidopsis genome using controlled vocabularies. Plant physiology 135: 745-755

Berendsen RL, van Verk MC, Stringlis IA, Zamioudis C, Tommassen J, Pieterse CM, Bakker PA (2015) Unearthing the genomes of plant-beneficial Pseudomonas model strains WCS358, WCS374 and WCS417. BMC genomics 16: 539

Bezrutczyk M, Yang J, Eom JS, Prior M, Sosso D, Hartwig T, Szurek B, Oliva R, Vera-Cruz C, White FF, Yang B, Frommer WB (2018) Sugar flux and signaling in plant-microbe interactions. The Plant journal : for cell and molecular biology 93: 675-685

Blom D, Fabbri C, Connor EC, Schiestl FP, Klauser DR, Boller T, Eberl L, Weisskopf L (2011) Production of plant growth modulating volatiles is widespread among rhizosphere bacteria and strongly depends on culture conditions. Environmental microbiology 13: 3047-3058

Bolger AM, Lohse M, Usadel B (2014) Trimmomatic: a flexible trimmer for Illumina sequence data. Bioinformatics 30: 2114-2120

Box MS, Coustham V, Dean C, Mylne JS (2011) Protocol: A simple phenol-based method for 96-well extraction of high quality RNA from Arabidopsis. Plant methods 7: 7

Chen L-Q (2014) SWEET sugar transporters for phloem transport and pathogen nutrition. New Phytologist 201: 1150-1155

Chen LQ, Hou BH, Lalonde S, Takanaga H, Hartung ML, Qu XQ, Guo WJ, Kim JG, Underwood W, Chaudhuri B, Chermak D, Antony G, White FF, Somerville SC, Mudgett MB, Frommer WB (2010) Sugar transporters for intercellular exchange and nutrition of pathogens. Nature 468: 527-532

Chen LQ, Lin IW, Qu XQ, Sosso D, McFarlane HE, Londono A, Samuels AL, Frommer WB (2015) A cascade of sequentially expressed sucrose transporters in the seed coat and endosperm provides nutrition for the Arabidopsis embryo. The Plant cell 27: 607-619

Chen LQ, Qu XQ, Hou BH, Sosso D, Osorio S, Fernie AR, Frommer WB (2012) Sucrose efflux mediated by SWEET proteins as a key step for phloem transport. Science 335: 207-211

Cheng CY, Krishnakumar V, Chan AP, Thibaud-Nissen F, Schobel S, Town CD (2017) Araport11: a complete reannotation of the Arabidopsis thaliana reference genome. The Plant journal : for cell and molecular biology 89: 789-804

Cole BJ, Feltcher ME, Waters RJ, Wetmore KM, Mucyn TS, Ryan EM, Wang G, Ul-Hasan S, McDonald M, Yoshikuni Y, Malmstrom RR, Deutschbauer AM, Dangl JL, Visel A (2017) Genome-wide identification of bacterial plant colonization genes. PLoS biology 15: e2002860

Czechowski T, Stitt M, Altmann T, Udvardi MK, Scheible WR (2005) Genome-wide identification and testing of superior reference genes for transcript normalization in Arabidopsis. Plant physiology 139: 5-17

De Coninck B, Le Roy K, Francis I, Clerens S, Vergauwen R, Halliday AM, Smith SM, Van Laere A & Van den Ende W (2005) *Arabidopsis* AtcwINV3 and 6 are not invertases but are fructan exohydrolases (FEHs) with different substrate specificities. Plant Cell Environ 28, 432– 443.

Duan Z, Homma A, Kobayashi M, Nagata N, Kaneko Y, Fujiki Y, Nishida I (2014) Photoassimilation, assimilate translocation and plasmodesmal biogenesis in the source leaves of Arabidopsis thaliana grown under an increased atmospheric CO2 concentration. Plant & cell physiology 55: 358-369

Durand M, Porcheron B, Hennion N, Maurousset L, Lemoine R, Pourtau N (2016) Water Deficit Enhances C Export to the Roots in Arabidopsis thaliana Plants with Contribution of Sucrose Transporters in Both Shoot and Roots. Plant physiology 170: 1460-1479

Eom JS, Chen LQ, Sosso D, Julius BT, Lin IW, Qu XQ, Braun DM, Frommer WB (2015) SWEETs, transporters for intracellular and intercellular sugar translocation. Current opinion in plant biology 25: 53-62

Gebauer P, Korn M, Engelsdorf T, Sonnewald U, Koch C, Voll LM (2017) Sugar Accumulation in Leaves of Arabidopsis sweet11/sweet12 Double Mutants Enhances Priming of the Salicylic Acid-Mediated Defense Response. Frontiers in plant science 8: 1378

Hennion N, Durand M, Vriet C, Doidy J, Maurousset L, Lemoine R, Pourtau N (2019) Sugars en route to the roots. Transport, metabolism and storage within plant roots and towards microorganisms of the rhizosphere. Physiologia plantarum 165: 44-57

Jauregui I, Aparicio-Tejo PM, Avila C, Rueda-Lopez M, Aranjuelo I (2015) Root and shoot performance of Arabidopsis thaliana exposed to elevated CO2: A physiologic, metabolic and transcriptomic response. Journal of plant physiology 189: 65-76

Kai M, Piechulla B (2009) Plant growth promotion due to rhizobacterial volatiles--an effect of CO2? FEBS letters 583: 3473-3477

Kanehisa M, Furumichi M, Tanabe M, Sato Y, Morishima K (2017) KEGG: new perspectives on genomes, pathways, diseases and drugs. Nucleic acids research 45: D353-D361

Kanehisa M, Goto S (2000) KEGG: kyoto encyclopedia of genes and genomes. Nucleic acids research 28: 27-30

Kim D, Langmead B, Salzberg SL (2015) HISAT: a fast spliced aligner with low memory requirements. Nature methods 12: 357-360

Kopylova E, Noe L, Touzet H (2012) SortMeRNA: fast and accurate filtering of ribosomal RNAs in metatranscriptomic data. Bioinformatics 28: 3211-3217

Le Hir R, Spinner L, Klemens PA, Chakraborti D, de Marco F, Vilaine F, Wolff N, Lemoine R, Porcheron B, Gery C, Teoule E, Chabout S, Mouille G, Neuhaus HE, Dinant S, Bellini C (2015) Disruption of the Sugar Transporters AtSWEET11 and AtSWEET12 Affects Vascular Development and Freezing Tolerance in Arabidopsis. Mol Plant 8: 1687-1690

Lemoine R, La Camera S, Atanassova R, Dedaldechamp F, Allario T, Pourtau N, Bonnemain JL, Laloi M, Coutos-Thevenot P, Maurousset L, Faucher M, Girousse C, Lemonnier P, Parrilla J, Durand M (2013) Source-to-sink transport of sugar and regulation by environmental factors. Frontiers in plant science 4: 272

Lemonnier P, Gaillard C, Veillet F, Verbeke J, Lemoine R, Coutos-Thevenot P, La Camera S (2014) Expression of Arabidopsis sugar transport protein STP13 differentially affects glucose transport activity and basal resistance to Botrytis cinerea. Plant molecular biology 85: 473-484

Li H, Handsaker B, Wysoker A, Fennell T, Ruan J, Homer N, Marth G, Abecasis G, Durbin R, 1000 Genome Project Data Processing Subgroup (2009) The Sequence Alignment/Map format and SAMtools. Bioinformatics 25: 2078-2079

Lobet G, Pages L, Draye X (2011) A novel image-analysis toolbox enabling quantitative analysis of root system architecture. Plant physiology 157: 29-39

Love MI, Huber W, Anders S (2014) Moderated estimation of fold change and dispersion for RNA-seq data with DESeq2. Genome biology 15: 550

Martin M (2011) Cutadapt Removes Adapter Sequences from High-Throughput Sequencing Reads. EMBnet Journal 17, 10-12.

Miotto-Vilanova L, Jacquard C, Courteaux B, Wortham L, Michel J, Clement C, Barka EA, Sanchez L (2016) Burkholderia phytofirmans PsJN Confers Grapevine Resistance against Botrytis cinerea via a Direct Antimicrobial Effect Combined with a Better Resource Mobilization. Frontiers in plant science 7: 1236

Pertea M, Pertea GM, Antonescu CM, Chang TC, Mendell JT, Salzberg SL (2015) StringTie enables improved reconstruction of a transcriptome from RNA-seq reads. Nature biotechnology 33: 290-295

Pieterse CM, Zamioudis C, Berendsen RL, Weller DM, Van Wees SC, Bakker PA (2014) Induced systemic resistance by beneficial microbes. Annual review of phytopathology 52: 347-375

Schmittgen TD, Livak KJ (2008) Analyzing real-time PCR data by the comparative C(T) method. Nature protocols 3: 1101-1108

Schneider CA, Rasband WS, Eliceiri KW (2012) NIH Image to ImageJ: 25 years of image analysis. Nature methods 9: 671-675

Schwachtje J, Karojet S, Thormahlen I, Bernholz C, Kunz S, Brouwer S, Schwochow M, Kohl K, van Dongen JT (2011) A naturally associated rhizobacterium of Arabidopsis thaliana induces a starvation-like transcriptional response while promoting growth. PloS one 6: e29382

Thimm O, Blasing O, Gibon Y, Nagel A, Meyer S, Kruger P, Selbig J, Muller LA, Rhee SY, Stitt M (2004) MAPMAN: a user-driven tool to display genomics data sets onto diagrams of metabolic pathways and other biological processes. The Plant journal : for cell and molecular biology 37: 914-939

Tsukanova, K., Chebotar, V., Meyer, J., & Bibikova, T. (2017). Effect of plant growth-promoting Rhizobacteria on plant hormone homeostasis. South African journal of botany, 113, 91-102.

Vacheron J, Desbrosses G, Bouffaud ML, Touraine B, Moenne-Loccoz Y, Muller D, Legendre L, Wisniewski-Dye F, Prigent-Combaret C (2013) Plant growth-promoting rhizobacteria and root system functioning. Frontiers in plant science 4: 356

Verhagen BW, Trotel-Aziz P, Couderchet M, Hofte M, Aziz A (2010) Pseudomonas spp.-induced systemic resistance to Botrytis cinerea is associated with induction and priming of defence responses in grapevine. Journal of experimental botany 61: 249-260

Wintermans PC, Bakker PA, Pieterse CM (2016) Natural genetic variation in Arabidopsis for responsiveness to plant growth-promoting rhizobacteria. Plant molecular biology 90: 623-634

Ye J, Coulouris G, Zaretskaya I, Cutcutache I, Rozen S, Madden TL (2012) Primer-BLAST: a tool to design target-specific primers for polymerase chain reaction. BMC bioinformatics 13: 134

Zamioudis C, Hanson J, Pieterse CM (2014) beta-Glucosidase BGLU42 is a MYB72-dependent key regulator of rhizobacteria-induced systemic resistance and modulates iron deficiency responses in Arabidopsis roots. The New phytologist 204: 368-379

Zamioudis C, Korteland J, Van Pelt JA, van Hamersveld M, Dombrowski N, Bai Y, Hanson J, Van Verk MC, Ling HQ, Schulze-Lefert P, Pieterse CM (2015) Rhizobacterial volatiles and photosynthesis-related signals coordinate MYB72 expression in Arabidopsis roots during onset of induced systemic resistance and iron-deficiency responses. The Plant journal : for cell and molecular biology 84: 309-322

Zamioudis C, Mastranesti P, Dhonukshe P, Blilou I, Pieterse CM (2013) Unraveling root developmental programs initiated by beneficial Pseudomonas spp. bacteria. Plant physiology 162: 304-318

FIGURES LEGENDS

Fig. 1. Phenotypic effects of *Pseudomonas simiae* WCS417r on *Arabidopsis thaliana* Col-0 seedlings 4, 7 and 10 days post inoculation (dpi). To study the phenotypic effects of *Ps*WCS417r in physical contact with the seedling roots, roots of five day old seedlings were either mock-treated ("Mock") or inoculated with *Ps*WCS417r ("WCS417r"). **a.** Left panels: pictures of whole seedlings (scale bar, 1cm). Right panels: macroscopy pictures of root tips (scale bar, 1 mm). **b.** Four, seven or ten days post inoculation, the root and shoot biomasses of the seedlings were measured and their root system architecture were analyzed. Data are means ± SEM of at least 9 biological replicates (n) from 3 independent experiments. Stars (stat. column) indicate statistically significant differences according to a Mann-Whitney-Wilcoxon test ns, non-significant ; *, P<0,05 ; **, P<0,01 ; ***, P<0,001).

Fig. 2. Differentially Expressed Genes in roots and shoots of *Arabidopsis thaliana* Col-0 seedlings 7 days post inoculation with *Pseudomonas simiae* WCS417r. a. Venn diagram of Differentially Expressed Genes (DEGs) in roots and shoots of *Arabidopsis thaliana* Col-0 seedlings 7 days post inoculation with *Ps*WCS417r. Differential gene expression analysis was performed on RNA-sequencing data. Genes whose expression was up-regulated (red arrow) or down-regulated (blue arrow) more than two fold and with a FDR < 0.05 were submitted to a Venn diagram analysis with pairwise comparisons between DEGs in root or shoot samples using the Venn Selector tool from the Bio-Analytic Resource for Plant Biology (https://bar.utoronto.ca/). **b.** Heatmap of DEGs involved in hormone biosynthesis and signaling pathways. List of genes were retrieved from the KEGG database: pathway ath04075 "Plant hormone signal transduction", for the plant hormone signaling pathways, and pathways ath00380 ("tryptophan metabolism"), ath00908 ("Zeatin metabolism"), ath00904 ("Diterpenoid biosynthesis"), ath00906 ("Carotenoid biosynthesis"), ath00270 ("Cysteine and methionine metabolism"), ath00905 ("Brassinosteroid biosynthesis"), ath00592 ("alpha-Linolenic acid metabolism"), and ath00360 ("Phenylalanine metabolism") for the plant hormone biosynthesis pathways (Auxin, Cytokinin, Gibberellin, Abscissic acid, Ethylene, Brassinosteroid, Jasmonic acid, and Salicylic acid, respectively). **c.** Heatmap of DEGs involved in plant-pathogen interactions. List of genes were retrieved from the KEGG database (pathway ath04626). **d.** Heatmap of DEGs involved in starch and sucrose metabolism. List of genes were retrieved from the KEGG database (pathway ath00500). Only Differentially Expressed Genes (DEGs) are shown in the heatmaps. Each color spot reflects

the differential expression level of the corresponding gene: red for up-regulated genes and blue for downregulated genes. Values on scale bar represent log2 fold changes.

Fig. 3. Effects of *Pseudomonas simiae* WCS417r on the relative expression of genes coding for sugar transporters in *Arabidopsis thaliana* Col-0 seedlings roots and shoots. Gene expression changes in roots and in shoots induced by *Ps*WCS417r in physical contact with the seedling roots 4, 7 and 10 days post inoculation (dpi) (**a**), or by *Ps*WCS417r volatile compounds at 7 dpi (**b**). Five day old seedlings were either mock-treated ("Mock") or treated with *Ps*WCS417r inoculum ("WCS417r"). Four, seven or ten days post inoculation, root and shoot tissues were harvested (at midday, 8h light) and transcript levels were quantified by qRT-PCR. The expression level of each gene was normalized to the reference gene At4g26410. Data are mean ± SEM of 4 to 6 biological replicates (pool of 30-60 seedlings each), each from an independent experiment. Stars indicate statistically significant differences according to a Mann-Whitney-Wilcoxon test (ns, non-significant ; *, P<0,05 ; **, P<0,01 ; ***, P<0,001). Fold change (Fc) values of gene expression are written in red for induction and in blue for repression in comparison to the mock. The present gene set corresponds to genes whose expression was induced or repressed more than 2 fold in the RNA-seq analysis (with FDR <0,05) and in a first qRT-PCR experiment performed with three biological replicates on all known sugar transporter genes in Arabidopsis (with a relative expression greater than 0.01) (Table S11).

Fig. 4. Phenotypic effects of *Pseudomonas simiae* WCS417r volatile compounds on *Arabidopsis thaliana* Col-0 WT, *sweet11*, *sweet12* and *sweet11/12* mutant seedlings 7 days post inoculation. Five day old seedlings were either mock-treated ("Mock") or exposed to *Ps*WCS417r volatile compounds ("WCS417r"). **a.** Pictures of whole seedlings (scale bar, 1cm). **b.** Macroscopy pictures of root tips (scale bar, 1 mm). **c.** Seven days post inoculation, the root and shoot biomasses of the seedlings were measured and their root system architecture were analyzed. Data are means ± SEM of 9 biological replicates (n) from 3 independent experiments. Stars (stat. column) indicate statistically significant differences between the "Mock" and "WCS417r" conditions for each genotype according to a Mann-Whitney-Wilcoxon test (ns: non significant; *, P < 0,05; **, P < 0,01; ***, P < 0,001). b letters above the bars indicate statistically significant differences between each mutant and the WT according to a Mann-Whitney test.

Fig. 5. Effects of *Pseudomonas simiae* WCS417r volatile compounds on the relative expression of genes coding for sugar transporters in roots (a) and shoots (b) of *Arabidopsis thaliana* Col-0 WT and *sweet11/sweet12* mutant seedlings 7 days post inoculation. Five day old seedlings were either mock-treated ("Mock") or exposed to *Ps*WCS417r volatile compounds ("WCS417r"). Seven days post inoculation, root and shoot tissues were harvested (at midday, 8h light) and transcript levels were quantified by qRT-PCR. The expression level of each gene was normalized to the reference gene At4g26410. Data are mean ± SEM of 4 biological replicates (pool of 30-40 seedlings each), each from an independent experiment. Stars indicate statistically significant differences according to Mann-Whitney-Wilcoxon test (ns, non-significant ; *, P<0,05 ; **, P<0,01 ; ***, P<0,001). Fold change (Fc) values are written in red for transcriptional induction and in blue transcriptional repression by WCS417r in comparison to the Mock. Letters above the bars indicate statistically significant differences between the genotypes according to a Mann-Whitney test, and their corresponding Fc is written in grey The data presented here correspond to a subset of genes whose relative expression levels were evaluated. The full set included genes with a relative expression greater than 0.01 and whose expression was induced or repressed more than 2 fold by WCS417r among all known sugar transporter genes in Arabidopsis, in addition to *SWEET* genes of the clade III in root and shoot, and three defense genes in shoot (Table S15).

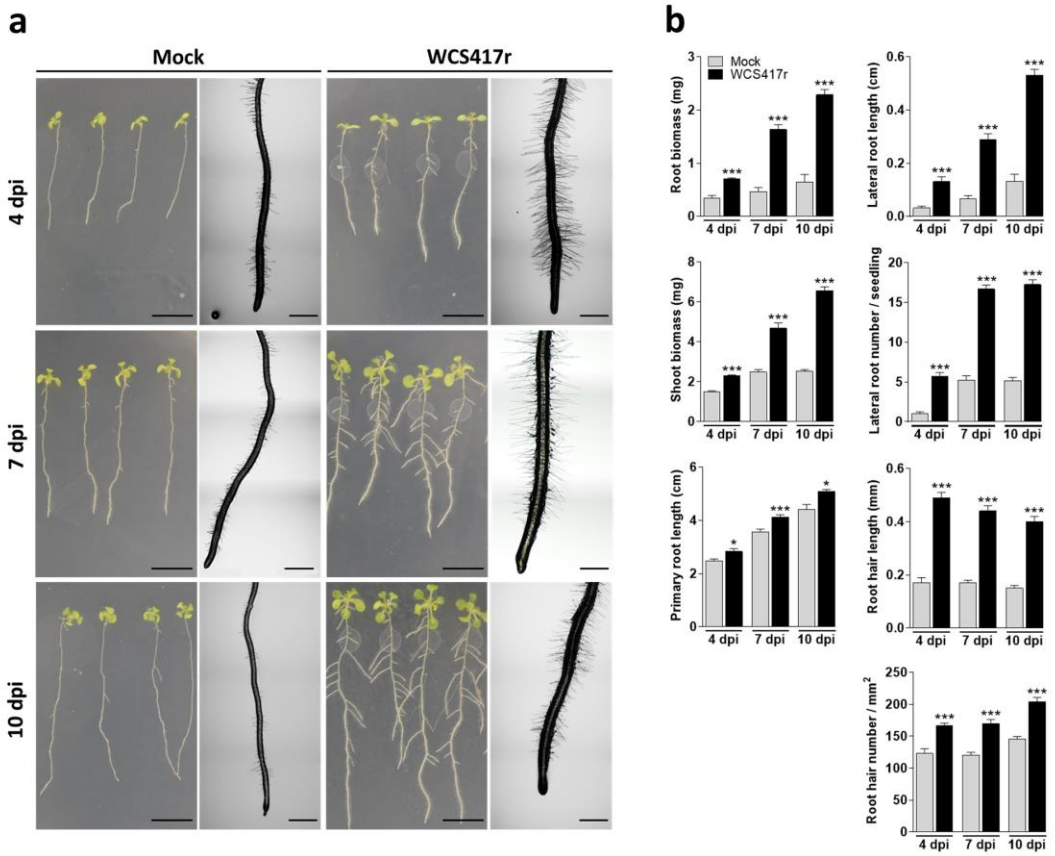

Fig. 1. Phenotypic effects of *Pseudomonas simiae* WCS417r on *Arabidopsis thaliana* Col-0 seedlings 4, 7 and 10 days post inoculation (dpi). To study the phenotypic effects of *Ps*WCS417r in physical contact with the seedling roots, roots of five day old seedlings were either mock-treated ("Mock") or inoculated with *Ps*WCS417r ("WCS417r"). **a.** Left panels: pictures of whole seedlings (scale bar, 1cm). Right panels: macroscopy pictures of root tips (scale bar, 1 mm). **b.** Four, seven or ten days post inoculation, the root and shoot biomasses of the seedlings were measured and their root system architecture were analyzed. Data are means ± SEM of at least 9 biological replicates (n) from 3 independent experiments. Stars (stat. column) indicate statistically significant differences according to a Mann-Whitney-Wilcoxon test ns, non-significant ; *, P<0,05 ; **, P<0,01 ; ***, P<0,001).

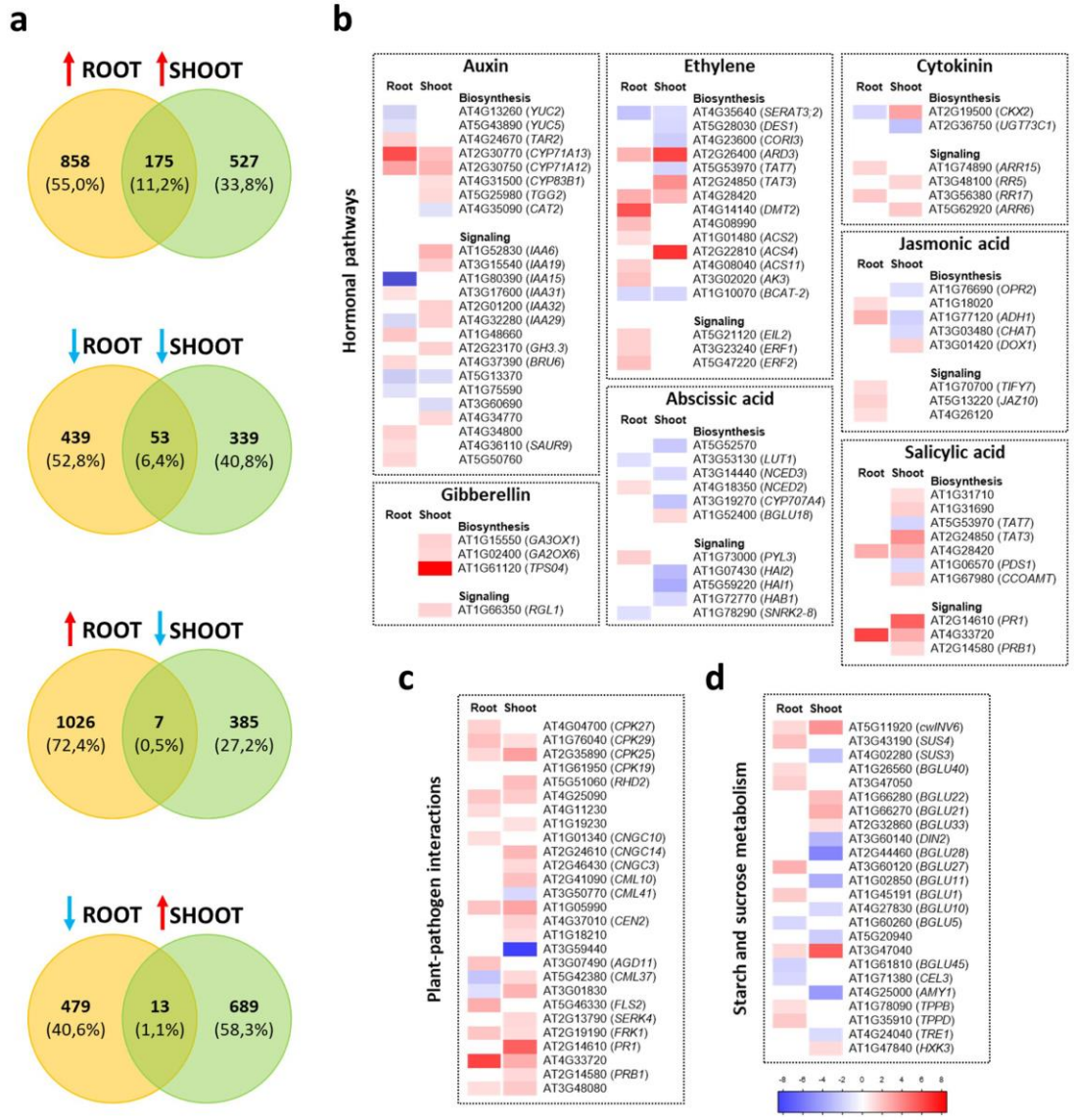

Fig. 2. Differentially Expressed Genes in roots and shoots of *Arabidopsis thaliana* Col-0 seedlings 7 days post inoculation with *Pseudomonas simiae* WCS417r. a. Venn diagram of Differentially Expressed Genes (DEGs) in roots and shoots of *Arabidopsis thaliana* Col-0 seedlings 7 days post inoculation with *Ps*WCS417r. Differential gene expression analysis was performed on RNA-sequencing data. Genes whose expression was up-regulated (red arrow) or down-regulated (blue arrow) more than two fold and with a FDR < 0.05 were submitted to a Venn diagram analysis with pairwise comparisons between DEGs in root or shoot samples using the Venn Selector tool from the Bio-Analytic Resource for Plant Biology (https://bar.utoronto.ca/). **b.** Heatmap of DEGs involved in hormone biosynthesis and signaling pathways. List of genes were retrieved from the KEGG database: pathway ath04075 "Plant hormone signal transduction", for the plant hormone signaling pathways, and pathways ath00380 ("tryptophan metabolism"), ath00908 ("Zeatin metabolism"), ath00904 ("Diterpenoid biosynthesis"), ath00906 ("Carotenoid biosynthesis"), ath00270 ("Cysteine and methionine metabolism"), ath00905 ("Brassinosteroid biosynthesis"), ath00592 ("alpha-Linolenic acid metabolism"), and ath00360 ("Phenylalanine metabolism") for the plant hormone biosynthesis pathways (Auxin, Cytokinin, Gibberellin, Abscissic acid, Ethylene, Brassinosteroid, Jasmonic acid, and Salicylic acid, respectively). **c.** Heatmap of DEGs involved in plant-pathogen interactions. List of genes were retrieved from the KEGG database (pathway ath04626). **d.** Heatmap of DEGs involved in starch and sucrose metabolism. List of genes were retrieved from the KEGG database (pathway ath00500). Only Differentially Expressed Genes (DEGs) are shown in the heatmaps. Each color spot reflects the differential expression level of the corresponding gene: red for up-regulated genes and blue for downregulated genes. Values on scale bar represent log2 fold changes.

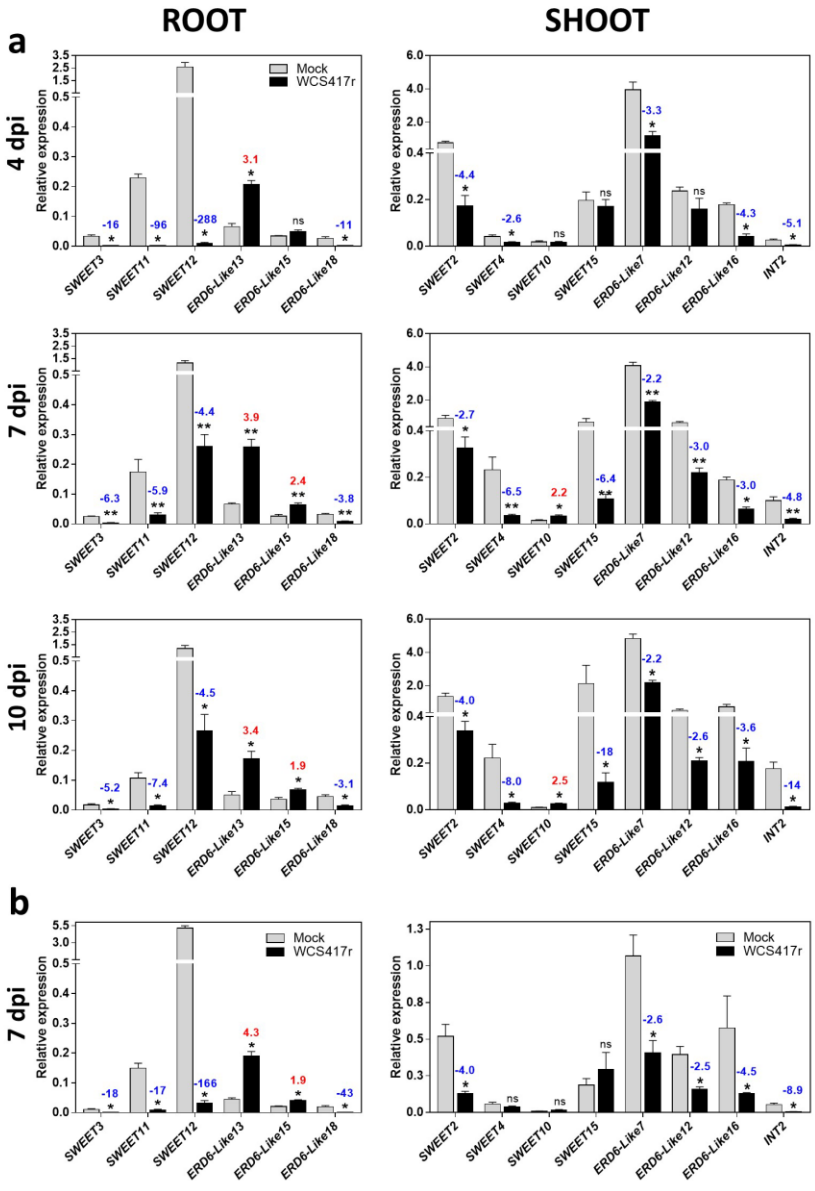

Fig. 3. Effects of *Pseudomonas simiae* WCS417r on the relative expression of genes coding for sugar transporters in *Arabidopsis thaliana* Col-0 seedlings roots and shoots. Gene expression changes in roots and in shoots induced by *Ps*WCS417r in physical contact with the seedling roots 4, 7 and 10 days post inoculation (dpi) (**a**), or by *Ps*WCS417r volatile compounds at 7 dpi (**b**). Five day old seedlings were either mock-treated ("Mock") or treated with *Ps*WCS417r inoculum ("WCS417r"). Four, seven or ten days post inoculation, root and shoot tissues were harvested (at midday, 8h light) and transcript levels were quantified by qRT-PCR. The expression level of each gene was normalized to the reference gene At4g26410. Data are mean ± SEM of 4 to 6 biological replicates (pool of 30-60 seedlings each), each from an independent experiment. Stars indicate statistically significant differences according to a Mann-Whitney-Wilcoxon test (ns, non-significant ; *, P<0,05 ; **, P<0,01 ; ***, P<0,001). Fold change (Fc) values of gene expression are written in red for induction and in blue for repression in comparison to the mock. The present gene set corresponds to genes whose expression was induced or repressed more than 2 fold in the RNA-seq analysis (with FDR <0,05) and in a first qRT-PCR experiment performed with three biological replicates on all known sugar transporter genes in Arabidopsis (with a relative expression greater than 0.01) (Table S11).

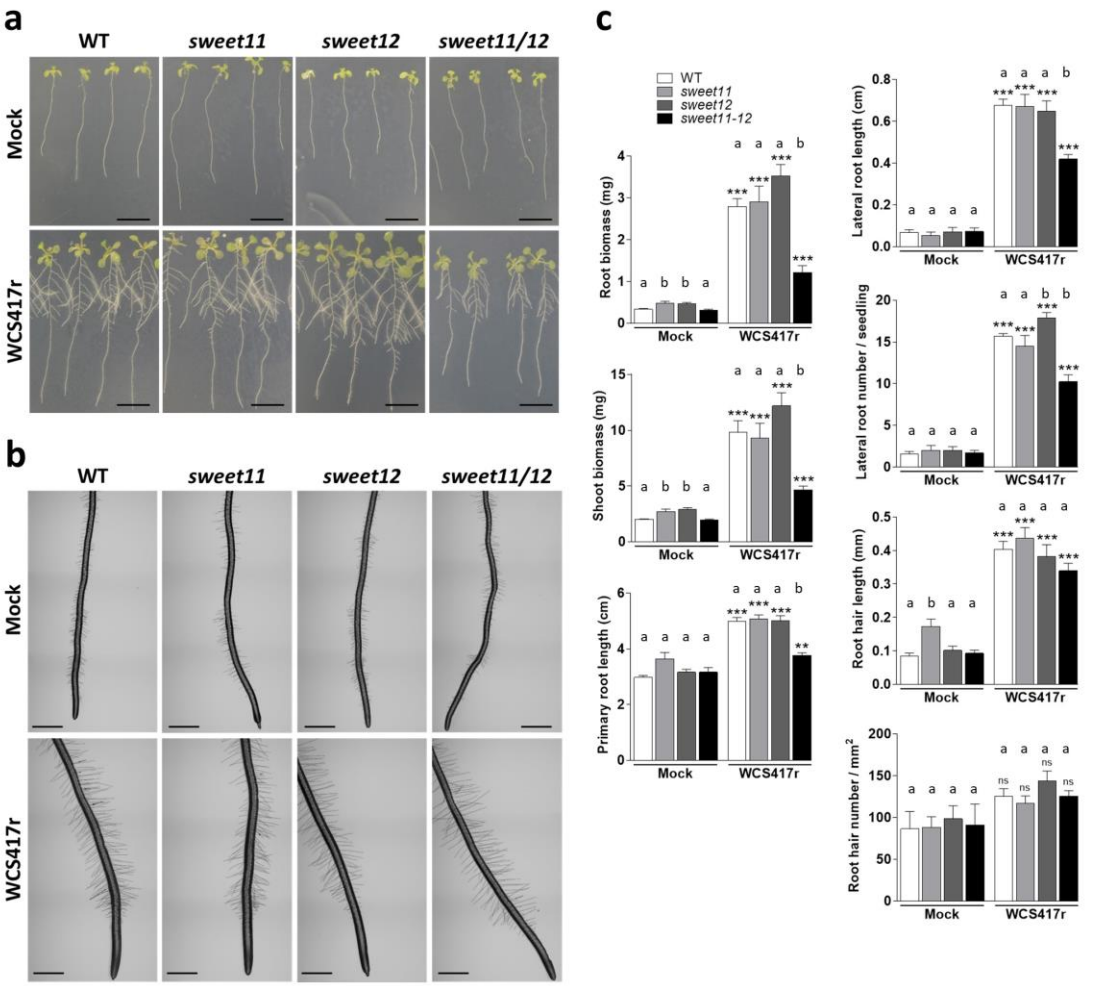

Fig. 4. Phenotypic effects of *Pseudomonas simiae* WCS417r volatile compounds on *Arabidopsis thaliana* Col-0 WT, *sweet11*, *sweet12* and *sweet11/12* mutant seedlings 7 days post inoculation. Five day old seedlings were either mock-treated ("Mock") or exposed to *Ps*WCS417r volatile compounds ("WCS417r"). **a.** Pictures of whole seedlings (scale bar, 1cm). **b.** Macroscopy pictures of root tips (scale bar, 1 mm). **c.** Seven days post inoculation, the root and shoot biomasses of the seedlings were measured and their root system architecture were analyzed. Data are means ± SEM of 9 biological replicates (n) from 3 independent experiments. Stars (stat. column) indicate statistically significant differences between the "Mock" and "WCS417r" conditions for each genotype according to a Mann-Whitney-Wilcoxon test (ns: non significant; *, $P < 0,05$; **, $P < 0,01$; ***, $P < 0,001$). b letters above the bars indicate statistically significant differences between each mutant and the WT according to a Mann-Whitney test.

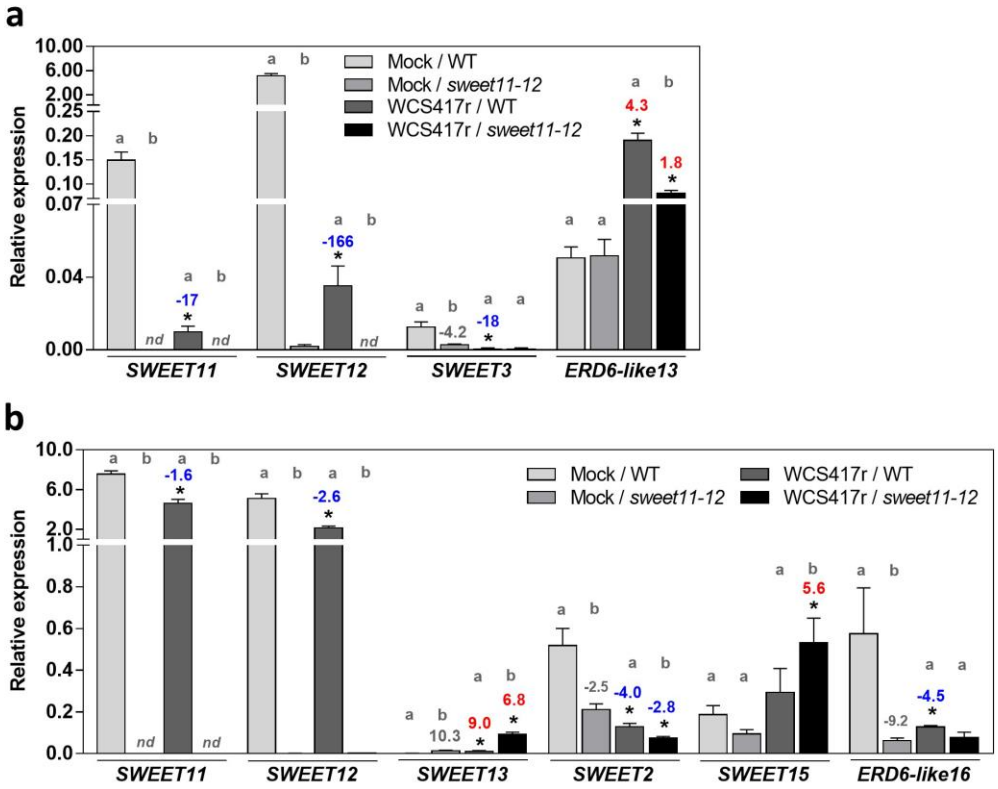

Fig. 5. Effects of *Pseudomonas simiae* WCS417r volatile compounds on the relative expression of genes coding for sugar transporters in roots (a) and shoots (b) of *Arabidopsis thaliana* Col-0 WT and *sweet11/sweet12* mutant seedlings 7 days post inoculation. Five day old seedlings were either mock-treated ("Mock") or exposed to *Ps*WCS417r volatile compounds ("WCS417r"). Seven days post inoculation, root and shoot tissues were harvested (at midday, 8h light) and transcript levels were quantified by qRT-PCR. The expression level of each gene was normalized to the reference gene At4g26410. Data are mean ± SEM of 4 biological replicates (pool of 30-40 seedlings each), each from an independent experiment. Stars indicate statistically significant differences according to Mann-Whitney-Wilcoxon test (ns, non-significant ; *, P<0,05 ; **, P<0,01 ; ***, P<0,001). Fold change (Fc) values are written in red for transcriptional induction and in blue transcriptional repression by WCS417r in comparison to the Mock. Letters above the bars indicate statistically significant differences between the genotypes according to a Mann-Whitney test, and their corresponding Fc is written in grey The data presented here correspond to a subset of genes whose relative expression levels were evaluated. The full set included genes with a relative expression greater than 0.01 and whose expression was induced or repressed more than 2 fold by WCS417r among all known sugar transporter genes in Arabidopsis, in addition to SWEET genes of the clade III in root and shoot, and three defense genes in shoot (Table S15).